

Superadiabatic stimulated Raman adiabatic passage between dressed states

Fangzhou Jin(金芳洲), Ao Wang(王奥), Yunlan Ji(季云兰), Hui Zhou(周辉), and Jianpei Geng(耿建培)
Citation: Chin. Phys. B, 2026, 35 (**1**): 010305. DOI: 10.1088/1674-1056/ade1c4
http://cpb.iphy.ac.cn; http://iopscience.iop.org/cpb

What follows is a list of articles you may be interested in

Efficient characterization of the coupler spectrum via sideband driving in superconducting qubits

Jianwen Xu(徐建文), Ruonan Guo(郭若男), Wen Zheng(郑文), Yu Zhang(张钰), Jie Zhao(赵杰), Zhiguo Huang(黄智国), Jingwei Wen(闻经纬), Runqing Zhang(张润清), Shaoxiong Li(李邵雄), Xinsheng Tan(谭新生), and Yang Yu(于扬)
Chin. Phys. B, 2025, 34 (**11**): 110302. DOI: 10.1088/1674-1056/ae00b0

Optimal multi-parameter quantum metrology for frequencies of magnetic field

Zhenhua Long(龙振华) and Shengshi Pang(庞盛世)
Chin. Phys. B, 2025, 34 (**8**): 080301. DOI: 10.1088/1674-1056/add4e7

Robust quantum gate optimization with first-order derivatives of ion-phonon and ion-ion couplings in trapped ions

Jing-Bo Wang(汪景波)
Chin. Phys. B, 2025, 34 (**4**): 040302. DOI: 10.1088/1674-1056/adb40e

Optimized pulse for stimulated Raman adiabatic passage on noisy experimental platform

Zhi-Ling Wang(王志凌), Leiyinan Liu(刘雷轶男), and Jian Cui(崔健)
Chin. Phys. B, 2021, 30 (**8**): 080305. DOI: 10.1088/1674-1056/abfccb

Fast generation of W state via superadiabatic-based shortcut in circuit quantum electrodynamics

Xue-Mei Wang(王雪梅), An-Qi Zhang(张安琪), Peng Xu(许鹏, and Sheng-Mei Zhao(赵生妹)
Chin. Phys. B, 2021, 30 (**3**): 030307. DOI: 10.1088/1674-1056/abd75b

---

Superadiabatic stimulated Raman adiabatic passage between dressed states

Fangzhou Jin(金芳洲)[1,†], Ao Wang(王奥)[1], Yunlan Ji(季云兰)[2], Hui Zhou(周辉)[2,‡], and Jianpei Geng(耿建培)[2,§]

[1] *Department of Fundamental Subjects, Wuchang Shouyi University, Wuhan* 430064, *China*
[2] *School of Physics, Hefei University of Technology, Hefei* 230009, *China*

(Received 17 April 2025; revised manuscript received 26 May 2025; accepted manuscript online 6 June 2025)

Stimulated Raman adiabatic passage (STIRAP) is a widely used technique for efficient population transfer between quantum states. However, the adiabatic nature of STIRAP requires slow evolution, leading to long operation times, which limits its practical applications. The superadiabatic method has been introduced to accelerate the STIRAP process, but it often necessitates additional couplings between the initial and target states, which may not be available in the original Hamiltonian. In this work, we present a novel approach to implement superadiabatic STIRAP (sa-STIRAP) between dressed states in a three-level quantum system. By modulating the amplitude and phase of the original driving fields, the initial and target states in dressed-state space can be effectively coupled. This approach provides a practical means of realizing sa-STIRAP in experimental setups, making it convenient to accelerate adiabatic quantum state transfer.

Keywords: superadiabatic, stimulated Raman adiabatic passage, quantum control, shortcuts to adiabaticity

PACS: 03.67.–a, 03.65.Vf, 42.50.–p

DOI: 10.1088/1674-1056/ade1c4 **CSTR:** 32038.14.CPB.ade1c4

1. Introduction

Stimulated Raman adiabatic passage (STIRAP)[1–3] has become a powerful method for the efficient transfer of population between quantum states, thanks to its robustness against spontaneous emission and its adaptability across diverse experimental conditions. Initially introduced in 1990,[1] STIRAP couples quantum states adiabatically via an intermediate state using two radiation fields, typically a pump and a Stokes field. This technique offers a significant advantage in quantum systems by ensuring high-fidelity population transfer while minimizing losses due to spontaneous emission. As a result, STIRAP has been widely adopted in various fields, ranging from physics and chemistry to broader applications in quantum technology.[3–8] Despite its considerable advantages, the adiabatic nature of STIRAP often necessitates slow evolution of the system, leading to long operation times. This slow evolution limits its applicability, especially in scenarios that require rapid state transfers.

To overcome this limitation, the concept of superadiabatic STIRAP (sa-STIRAP)[9,10] has been introduced, aiming to accelerate the population transfer process while preserving the high fidelity of adiabatic transitions. The superadiabatic approach involves the application of counterdiabatic driving techniques[11–18] to modify the standard STIRAP protocol. These techniques often incorporate additional couplings between the initial and target states, enabling faster evolution of the system, thereby reducing operation times without compromising transfer efficiency. However, implementing sa-STIRAP typically requires the introduction of auxiliary couplings that may not be naturally present in the system's Hamiltonian, posing challenges for experimental realization.[17,19] There has been numerous researches aimed at realizing sa-STIRAP, including methods such as applying invariant-based inverse engineering to the three-level system,[20–24] using two-photon transition superadiabatic passages,[25–28] and mapping or approximating the three-level system to a specific model.[19,20,30]

In this paper, we propose an alternative approach for implementing sa-STIRAP between dressed states in a three-level quantum system. Dressed states, which arise from the interaction of quantum systems with external fields, offer a robust structure that enhances coherence protection for improved quantum task performance.[31–42] By modulating the amplitude and phase of the driving fields, we demonstrate that it is possible to effectively couple the initial and target states within the dressed-state space, facilitating superadiabatic transfer without requiring additional couplings. This approach offers a practical means to accelerate adiabatic population transfer in quantum systems, making sa-STIRAP more accessible for experimental implementation. Our approach has the potential to improve the speed and efficiency of adiabatic quantum state transfer, opening new avenues for quantum control and other quantum technologies.

†Corresponding author. E-mail: fzjin@wsyu.edu.cn
‡Corresponding author. E-mail: zhouhui9240@163.com
§Corresponding author. E-mail: jianpei.geng@hfut.edu.cn

© 2026 Chinese Physical Society and IOP Publishing Ltd. All rights, including for text and data mining, AI training, and similar technologies, are reserved.

The paper is organized as follows. Section 2 provides an overview of STIRAP and superadiabatic STIRAP in a three-level system. Section 3 explores the concept of STIRAP between dressed states. In Section 4, we present our proposed method for implementing sa-STIRAP between dressed states. Finally, Section 5 concludes with a summary of our findings and potential directions for future work.

2. STIRAP and sa-STIRAP in three level system

The STIRAP protocol[2,3] is considered in a three-level system with a set of energy eigenstates $\{|1\rangle, |2\rangle, |3\rangle\}$, corresponding to the energy eigenvalues E_1, E_2, and E_3, respectively. The transitions $|1\rangle \leftrightarrow |2\rangle$ and $|2\rangle \leftrightarrow |3\rangle$ are allowed, as shown in Fig. 1(a). These states form a V-type configuration in which the states $|1\rangle$ and $|3\rangle$ to the ancillary level $|2\rangle$ are driven by external control fields with the frequency $\omega_1 = (E_1 - E_2)/\hbar - \Delta$ and $\omega_2 = (E_3 - E_2)/\hbar - \Delta$, where $\hbar$ is the reduced Planck constant. For simplicity, we adopt the convention $\hbar = 1$ throughout the rest of this paper. The Rabi frequencies of the two control fields are time-dependent and are denoted by $\Omega_{\rm p}(t)$ and $\Omega_{\rm s}(t)$. The objective of STIRAP is to achieve population transfer between the states $|1\rangle$ and $|3\rangle$, which are indirectly coupled via the intermediate state $|2\rangle$ while avoiding any population buildup in state $|2\rangle$. In the rotating frame and under the rotating wave approximation, the Hamiltonian for this three-level system is given by

$$H_0(t) = \begin{pmatrix} 0 & \frac{\Omega_{\rm p}(t)}{2} & 0 \\ \frac{\Omega_{\rm p}(t)}{2} & \Delta & \frac{\Omega_{\rm s}(t)}{2} \\ 0 & \frac{\Omega_{\rm s}(t)}{2} & 0 \end{pmatrix}, \tag{1}$$

where Δ is the detuning. The instantaneous eigenstates of $H_0(t)$ are

$$\begin{aligned} |n_0\rangle &= \cos\theta|1\rangle - \sin\theta|3\rangle, \\ |n_+\rangle &= \sin\theta\sin\alpha|1\rangle + \cos\alpha|2\rangle + \cos\theta\sin\alpha|3\rangle, \\ |n_-\rangle &= \sin\theta\cos\alpha|1\rangle - \sin\alpha|2\rangle + \cos\theta\cos\alpha|3\rangle, \end{aligned} \tag{2}$$

where $\tan\theta = \Omega_{\rm p}(t)/\Omega_{\rm s}(t)$, and $\tan(2\alpha) = \Omega/\Delta$, with $\Omega = \sqrt{\Omega_{\rm p}^2(t) + \Omega_{\rm s}^2(t)}$. The state $|n_0\rangle$ is the dark state with instantaneous eigenvalue zero. If the system is prepared in the initial state $|n_0(t_i)\rangle = |1\rangle$, and the evolution proceeds adiabatically, the global condition for adiabatic evolution is given by $\Omega_{\rm m}\delta t \gg 1$,[2] where $\Omega_{\rm m}$ is the peak amplitude of both $\Omega_{\rm p}(t)$ and $\Omega_{\rm s}(t)$, and δt is the time delay between these pulses. Under these conditions, the system will always remain in the dark state throughout its evolution. By maintaining the condition $\Omega_{\rm p}(t_i)/\Omega_{\rm s}(t_i) \approx 0$ at the initial time t_i, and $\Omega_{\rm s}(t_{\rm f})/\Omega_{\rm p}(t_{\rm f}) \approx 0$ at the final time $t_{\rm f}$, the system will evolve adiabatically into the final state $|n_0(t_{\rm f})\rangle = |3\rangle$, without ever populating the intermediate state $|2\rangle$.

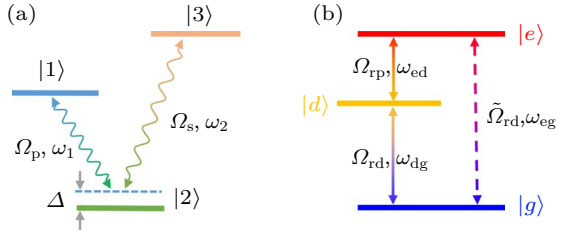


Fig. 1. (a) A three-level system characterized by orthonormal basis states $|1\rangle$, $|2\rangle$, and $|3\rangle$, with allowed transitions $|1\rangle \leftrightarrow |2\rangle$ and $|2\rangle \leftrightarrow |3\rangle$. (b) The dressed states of the driven system depicted in panel (a), where $\omega_{\rm ed}$, $\omega_{\rm dg}$, and $\omega_{\rm eg}$ represent the corresponding energy gaps. Transitions between the dressed states $\{|e\rangle, |d\rangle, |g\rangle\}$ can be realized by modulating the amplitude and phase of the original driving fields.

The adiabatic nature of STIRAP requires a slow evolution, which leads to long operation times, thus limiting its practical applications, particularly in the presence of decoherence. To speed up the STIRAP transfer, that is, to quickly transition from $|1\rangle \to |3\rangle$, superadiabatic driving can be employed.[11–13] The sa-STIRAP approach assumes a total control Hamiltonian for the three-level system, which takes the form[10]

$$H_1(t) = H_0(t) + H_{\rm s}(t), \tag{3}$$

where $H_{\rm s}(t)$ represents the additional superadiabatic correction Hamiltonian, given by

$$H_{\rm s}(t) = {\rm i}\sum_n [|\partial_t n\rangle\langle n| - \langle n|\partial_t n\rangle|n\rangle\langle n|]. \tag{4}$$

Here, $|n\rangle$ refers to the three instantaneous eigenstates $\{|n_0\rangle, |n_+\rangle, |n_-\rangle\}$. And $H_{\rm s}(t)$ can be calculated to the following simple expression:[10]

$$H_{\rm s}(t) = {\rm i}\Omega_{\rm d}(t)|1\rangle\langle 3| + {\rm H.c.}, \tag{5}$$

where $\Omega_{\rm d}(t)$ is given by

$$\Omega_{\rm d}(t) = \frac{\dot{\Omega}_{\rm p}(t)\Omega_{\rm s}(t) - \Omega_{\rm p}(t)\dot{\Omega}_{\rm s}(t)}{\Omega_{\rm p}^2(t) + \Omega_{\rm s}^2(t)}. \tag{6}$$

This term $H_{\rm s}(t)$ represents an additional coupling between the states $|1\rangle$ and $|3\rangle$, which can effectively suppress diabatic transitions. However, implementing such a coupling may be challenging or impractical in some systems due to selection rules arising from the symmetry of the states or the required phase conditions.[17] In the following, we introduce a novel approach to implement sa-STIRAP between dressed states in a three-level quantum system, enabling efficient coupling between the initial and target states.

3. STIRAP between dressed states

We now proceed to implement STIRAP between the dressed states in a three-level system. As shown in Fig. 1(a), the nonzero detuning Δ and the Rabi frequencies $\Omega_{\rm p}$ and $\Omega_{\rm s}$

of the two driving fields are held constant at Ω_0. The Hamiltonian in the rotating frame, under the rotating wave approximation, is given by

$$H_2 = \Delta|2\rangle\langle 2| + \frac{\Omega_0}{2}|1\rangle\langle 2| + \frac{\Omega_0}{2}|2\rangle\langle 3| + \text{H.c.} \tag{7}$$

The eigenstates of H_2 include a dark state $|d\rangle$ and dressed states $|e\rangle$ and $|g\rangle$, defined as[34,42]

$$\begin{aligned} |d\rangle &= (|1\rangle - |3\rangle)/\sqrt{2}, \\ |e\rangle &= \sin\beta\ |2\rangle + \cos\beta\ |b\rangle, \\ |g\rangle &= -\cos\beta\ |2\rangle + \sin\beta\ |b\rangle, \end{aligned} \tag{8}$$

where $|b\rangle$ is the bright state as $|b\rangle = (|1\rangle + |3\rangle)/\sqrt{2}$, and $\tan(2\beta) = \sqrt{2}\,\Omega_0/\Delta$. The corresponding eigenvalues are $\omega_{\rm d} = \Delta$ and $\omega_{\rm e,g} = (\Delta \pm \sqrt{\Delta^2 + 2\Omega_0^2})/2$. Thus, $|d\rangle$, $|e\rangle$, and $|g\rangle$ form a new three-level system. In this dressed-state space, we take $|e\rangle$ as the initial state and $|g\rangle$ as the target state, with $|d\rangle$ serving as an intermediate state. By introducing external control fields $\Omega_{\rm rp}(t)$ and $\Omega_{\rm rs}(t)$ for the transitions $|e\rangle \leftrightarrow |d\rangle$ and $|d\rangle \leftrightarrow |g\rangle$ in this three-level system,[42] as illustrated in Fig. 1(b), we can realize STIRAP between the dressed states. The details of this process are discussed in the following text.

We begin by considering the original Hamiltonian in the laboratory frame, which is given by

$$\begin{aligned} H_3(t) &= E_1|1\rangle\langle 1| + E_2|2\rangle\langle 2| + E_3|3\rangle\langle 3| \\ &\quad + \sqrt{2}\Omega_0[\cos(\omega_1 t + \varphi_1(t)) \\ &\quad + \cos(\omega_2 t + \varphi_2(t))]S_x, \end{aligned} \tag{9}$$

where S_x is the Pauli-x matrix for a spin-1 system, $\omega_1 = E_1 - E_2 - \Delta$ and $\omega_2 = E_3 - E_2 - \Delta$ represent the frequencies of the two driving fields. The time-dependent phase variations of the driving fields are denoted by $\varphi_1(t)$ and $\varphi_2(t)$. Next, we transform this Hamiltonian to the rotating frame using the unitary operator $U_{\rm r}$, and apply the rotating wave approximation to obtain the Hamiltonian in the rotating frame

$$\begin{aligned} H_4(t) &= U_{\rm r}H_3(t)U_{\rm r}^\dagger - {\rm i}U_{\rm r}\frac{{\rm d}U_{\rm r}^\dagger}{{\rm d}t} \\ &= [\Delta - \dot{\varphi}_1(t)]|1\rangle\langle 1| + [\Delta - \dot{\varphi}_2(t)]|3\rangle\langle 3| + \frac{\Omega_0}{2}S_x, \end{aligned} \tag{10}$$

where

$$U_{\rm r} = \exp\left(\frac{{\rm i}[\omega_1 t + \varphi_1(t)]}{2}(S_z^2 + S_z) + \frac{{\rm i}[\omega_2 t + \varphi_2(t)]}{2}(S_z^2 - S_z)\right).$$

This transformation rotates the system's states and operators to match the oscillatory part of the Hamiltonian, effectively eliminating fast-oscillating terms. When averaged over time, these terms simplify, resulting in a more tractable Hamiltonian. The Pauli matrices S_x and S_z for spin-1 system are defined as

$$S_x = \frac{1}{\sqrt{2}}\begin{pmatrix} 0 & 1 & 0 \\ 1 & 0 & 1 \\ 0 & 1 & 0 \end{pmatrix}, \quad S_z = \begin{pmatrix} 1 & 0 & 0 \\ 0 & 0 & 0 \\ 0 & 0 & -1 \end{pmatrix}. \tag{11}$$

The time-dependent phase variations are assumed to follow the form

$$\begin{aligned} \varphi_1(t) &= -\frac{\Omega_{\rm rp}(t)\sin(\omega_{\rm ed}t)}{\omega_{\rm ed}\cos\beta} - \frac{\Omega_{\rm rs}(t)\sin(\omega_{\rm dg}t)}{\omega_{\rm dg}\sin\beta}, \\ \varphi_2(t) &= \frac{\Omega_{\rm rp}(t)\sin(\omega_{\rm ed}t)}{\omega_{\rm ed}\cos\beta} + \frac{\Omega_{\rm rs}(t)\sin(\omega_{\rm dg}t)}{\omega_{\rm dg}\sin\beta}. \end{aligned} \tag{12}$$

Here, $\beta = \arctan(\sqrt{2}\ \Omega_0/\Delta)/2$, $\omega_{\rm ed} = \omega_{\rm e} - \omega_{\rm d}$ and $\omega_{\rm dg} = \omega_{\rm d} - \omega_{\rm g}$ represent the frequency differences between the respective levels. Now, we rewrite the Hamiltonian in the dressed-state basis using the transformation $U_{\rm d}$, then,

$$\begin{aligned} H_5(t) &= U_{\rm d}^\dagger H_4(t)U_{\rm d} \\ &= \omega_{\rm e}|e\rangle\langle e| + \omega_{\rm d}|d\rangle\langle d| + \omega_{\rm g}|g\rangle\langle g| + [\Omega_{\rm rp}(t)\cos(\omega_{\rm ed}t) \\ &\quad + \Omega_{\rm rs}(t)\cos(\omega_{\rm dg}t)\cot(\beta)]|e\rangle\langle d| \\ &\quad + [\Omega_{\rm rp}(t)\cos(\omega_{\rm ed}t)\tan(\beta) \\ &\quad + \Omega_{\rm rs}(t)\cos(\omega_{\rm dg}t)]|d\rangle\langle g| + \text{H.c.}, \end{aligned} \tag{13}$$

where $U_{\rm d}$ is the transformation matrix

$$\begin{aligned} U_{\rm d} &= \{|e\rangle, |d\rangle, |g\rangle\} \\ &= \frac{1}{\sqrt{2}}\begin{pmatrix} \cos\beta & 1 & \sin\beta \\ \sqrt{2}\sin\beta & 0 & -\sqrt{2}\cos\beta \\ \cos\beta & -1 & \sin\beta \end{pmatrix}. \end{aligned} \tag{14}$$

Since the control field at $\omega_{\rm ed}$ (resonant with the transition $|e\rangle \leftrightarrow |d\rangle$) and $\omega_{\rm dg}$ (resonant with the transition $|d\rangle \leftrightarrow |g\rangle$) are far off-resonant with the other transitions, we can simplify the Hamiltonian by retaining only the resonant terms. This gives us the following approximation:

$$\begin{aligned} H_6(t) &= \omega_{\rm e}|e\rangle\langle e| + \omega_{\rm d}|d\rangle\langle d| + \omega_{\rm g}|g\rangle\langle g| \\ &\quad + \Omega_{\rm rp}(t)\cos(\omega_{\rm ed}t)|e\rangle\langle d| \\ &\quad + \Omega_{\rm rs}(t)\cos(\omega_{\rm dg}t)|d\rangle\langle g| + \text{H.c.} \end{aligned} \tag{15}$$

In the rotating frame and applying the rotating wave approximation, we obtain the final Hamiltonian in the dressed-state space

$$H_7(t) = \frac{\Omega_{\rm rp}(t)}{2}|e\rangle\langle d| + \frac{\Omega_{\rm rs}(t)}{2}|d\rangle\langle g| + \text{H.c.}, \tag{16}$$

where the time-dependent parameters $\Omega_{\rm rp}(t)$ and $\Omega_{\rm rs}(t)$, derived from the phase terms in Eq. (12), serve as the driving field in the dressed subspace.

The Hamiltonian $H_7(t)$ has an instantaneous eigenstate, the dark state $|D(t)\rangle$, which corresponds to an eigenvalue of zero

$$|D(t)\rangle = \cos\theta_{\rm r}|e\rangle - \sin\theta_{\rm r}|g\rangle, \tag{17}$$

where $\tan\theta_{\rm r} = \Omega_{\rm rp}(t)/\Omega_{\rm rs}(t)$. If the system is initially prepared in the state $|D(t_i)\rangle = |e\rangle$, and the evolution proceeds adiabatically, the system will remain in the dark state throughout

the evolution. By maintaining the condition $\Omega_{\rm rp}(t_i)/\Omega_{\rm rs}(t_i) \approx 0$ at the initial time t_i, and $\Omega_{\rm rs}(t_{\rm f})/\Omega_{\rm rp}(t_{\rm f}) \approx 0$ at the final time $t_{\rm f}$, the system will evolve adiabatically into the final state $|D(t_{\rm f})\rangle = |g\rangle$, thereby implementing STIRAP between the dressed states.

Next, we numerically simulate the STIRAP process using both Gaussian pulses[2,19] and Vitanov-style pulses.[21,43] The Gaussian pulses are defined as

$$\Omega_{\rm rp}(t) = \Omega_{\rm r0}\exp\left(-\frac{(t-\frac{t_{\rm f}}{2}-t_0)^2}{\tau^2}\right),$$
$$\Omega_{\rm rs}(t) = \Omega_{\rm r0}\exp\left(-\frac{(t-\frac{t_{\rm f}}{2}+t_0)^2}{\tau^2}\right), \tag{18}$$

where the parameters are $t_{\rm f} = 10$ μs, and $t_0 = t_{\rm f}/10$, $\tau = t_{\rm f}/6$, as shown in Fig. 2(a). For the Vitanov-style pulses, the expressions are given by

$$\widetilde{\Omega}_{\rm rp}(t) = \Omega_{\rm r0}\ \sin\left(\frac{\pi}{2}\frac{1}{1+{\rm e}^{-(t-t_{\rm f})/\widetilde{\tau}}}\right),$$
$$\widetilde{\Omega}_{\rm rs}(t) = \Omega_{\rm r0}\ \cos\left(\frac{\pi}{2}\frac{1}{1+{\rm e}^{-(t-t_{\rm f})/\widetilde{\tau}}}\right), \tag{19}$$

where $t_{\rm f} = 10$ μs, and $\widetilde{\tau} = t_{\rm f}/10$, as illustrated in Fig. 2(b).

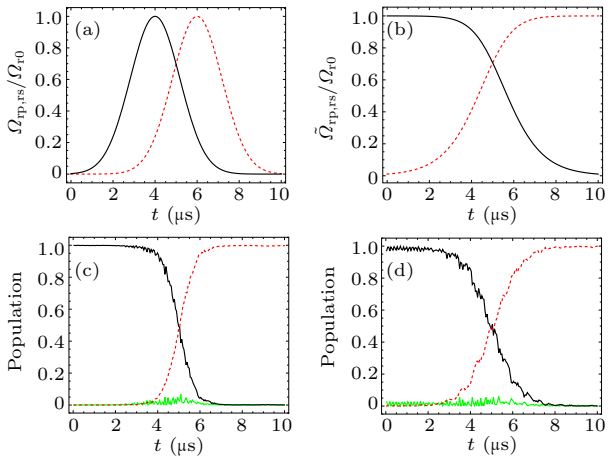


Fig. 2. (a) The Gaussian pulses have the following parameters: $t_{\rm f} = 10$ μs, and $t_0 = t_{\rm f}/10$, $\tau = t_{\rm f}/6$. (b) The Vitanov-style pulses are characterized by $t_{\rm f} = 10$ μs, and $\widetilde{\tau} = t_{\rm f}/10$. In both panels (a) and (b), the dashed red line represents the shape of pump pulses ($\Omega_{\rm rp}/\Omega_{\rm r0}$ or $\widetilde{\Omega}_{\rm rp}/\Omega_{\rm r0}$), while the solid black line represents the shape of Stokes pulses ($\Omega_{\rm rs}/\Omega_{\rm r0}$ or $\widetilde{\Omega}_{\rm rs}/\Omega_{\rm r0}$). Panels (c) and (d) show the state evolutions during STIRAP. The solid black line represents the population of the state $|e\rangle$, the dashed red line represents the population of the state $|g\rangle$, and the green line represents the population of the state $|d\rangle$. Panel (c) presents the results for Gaussian pulses, while panel (d) displays the results for Vitanov-style pulses. The population is defined as $|\langle m|\psi(t)\rangle|^2$, where $|m\rangle \in \{|e\rangle, |d\rangle, |g\rangle\}$. The parameters used in the calculations are as follows: $E_1 = 5$ GHz, $E_2 = 0$, $E_3 = 10$ GHz, $\Omega_0 = 200$ MHz, $\Delta = 200$ MHz, and $\Omega_{\rm r0} = 20$ MHz.

We perform numerical calculations using the original Hamiltonian $H_3(t)$ (i.e., Eq. (9)) in the laboratory frame without any approximations. The system is initially in the state $|\psi(0)\rangle = |e\rangle$ at $t = 0$, and the final state at $t = t_{\rm f}$ is given by $|\psi(t_{\rm f})\rangle = U_{\rm r}\exp[-{\rm i}\int_0^{t_{\rm f}} H_3(t)\,{\rm d}t]|e\rangle$. This approach decomposes the unitary evolution into products of small time intervals Δt , and takes the limit as $\Delta t \to 0$. The parameters used in the calculations are as follows: $E_1 = 5$ GHz, $E_2 = 0$, $E_3 = 10$ GHz, $\Omega_0 = 200$ MHz, $\Delta = 200$ MHz, and $\Omega_{\rm r0} = 20$ MHz. The results for STIRAP using Gaussian pulses and Vitanov-style pulses are shown in Figs. 2(c) and 2(d), respectively. These results clearly demonstrate that the system, initially in the state $|e\rangle$, can undergo an adiabatic transfer to the final state $|g\rangle$. When $t_{\rm f} = 1$ μs, the adiabatic condition is not well satisfied, leading to an incomplete STIRAP process, as shown in Figs. 3(a) and 3(b). The lines in these figures are non-smooth due to the numerical calculations performed without the rotating wave approximation.

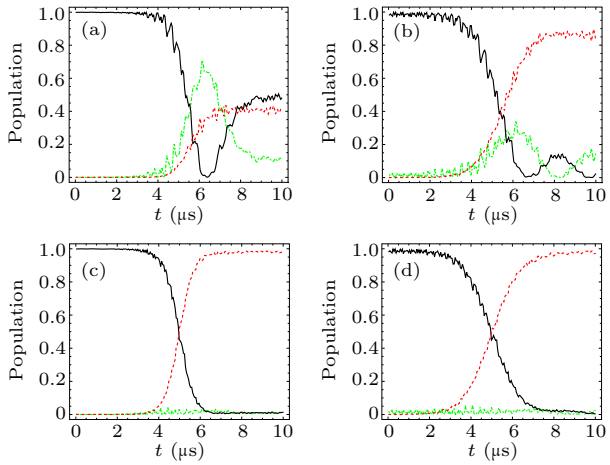


Fig. 3. The parameter $t_{\rm f}$ is set to $t_{\rm f} = 1$ μs, and the other parameters used in the calculations are the same as those in Fig. 2. The results are as follows: (a) STIRAP process using Gaussian pulses, (b) STIRAP process using Vitanov-style pulses, (c) sa-STIRAP process using Gaussian pulses, (d) sa-STIRAP process using Vitanov-style pulses. In each panel, the solid black line represents the population of the state $|e\rangle$, the dashed red line represents the population of the state $|g\rangle$, and the green line represents the population of the state $|d\rangle$.

4. Superadiabatic STIRAP between dressed states

To accelerate the STIRAP transfer between dressed states, specifically to transition from $|e\rangle$ to $|g\rangle$, superadiabatic driving can be employed. In general, superadiabatic control requires an additional coupling between the initial and target states, which effectively suppresses diabatic transitions.[10] By modulating the amplitude and phase of the original driving fields, we can create an effective coupling between the initial and target states in the dressed-state space. Starting with the original Hamiltonian in the laboratory frame $H_3(t)$, we introduce a new driving field. The Hamiltonian then becomes

$$H_8(t) = H_3(t) + H_{\rm sa}(t), \tag{20}$$

where

$$H_{\rm sa}(t) = \sqrt{2}\Omega_{\rm rd}(t)\left[\cos\left(\omega_1 t + \varphi_1(t) + \frac{\pi}{2}\right) + \cos\left(\omega_2 t + \varphi_2(t) + \frac{\pi}{2}\right)\right]S_x. \tag{21}$$

Applying the rotating wave approximation in the rotating frame and transforming to the dressed-state basis, the first term

$H_3(t)$ is given by Eq. (16). We now detail the transformation process of $H_{\rm sa}(t)$. First, we transform $H_{\rm sa}(t)$ to the rotating frame using the unitary operator $U_{\rm r}$ and apply the rotating wave approximation to obtain

$$H_{\rm sa1}(t) = -\frac{\rm i}{2}\Omega_{\rm rd}(t)|1\rangle\langle 2| + \frac{\rm i}{2}\Omega_{\rm rd}(t)|2\rangle\langle 3| + {\rm H.c.} \quad (22)$$

Next, we rewrite the Hamiltonian in the dressed-state basis using the transformation $U_{\rm d}$

$$H_{\rm sa2}(t) = U_{\rm d}^{\dagger}H_{\rm sa1}(t)U_{\rm d} = \frac{\rm i}{\sqrt{2}}\Omega_{\rm rd}(t)|e\rangle\langle g| + {\rm H.c.} \quad (23)$$

We set $\Omega_{\rm rd}(t) = 2\sqrt{2}\widetilde{\Omega}_{\rm rd}(t)\cos(\omega_{\rm eg}t)$, where $\omega_{\rm eg} = \omega_{\rm e} - \omega_{\rm g}$, and apply the rotating wave approximation. The Hamiltonian becomes

$$H_{\rm sa3}(t) = {\rm i}\widetilde{\Omega}_{\rm rd}(t)|e\rangle\langle g| + {\rm H.c.} \quad (24)$$

Finally, the total Hamiltonian $H_8(t)$ becomes

$$\begin{aligned} H_9(t) \;=\; & \frac{\Omega_{\rm rp}(t)}{2}|e\rangle\langle d| + \frac{\Omega_{\rm rs}(t)}{2}|d\rangle\langle g| \\ & + {\rm i}\widetilde{\Omega}_{\rm rd}(t)|e\rangle\langle g| + {\rm H.c.}, \end{aligned} \quad (25)$$

where the term ${\rm i}\widetilde{\Omega}_{\rm rd}(t)|e\rangle\langle g|$ represents the effective coupling between $|e\rangle$ and $|g\rangle$. To ensure the superadiabatic driving is properly satisfied, we define $\widetilde{\Omega}_{\rm rd}(t)$ as

$$\widetilde{\Omega}_{\rm rd}(t) = \frac{\dot{\Omega}_{\rm rp}(t)\Omega_{\rm rs}(t) - \Omega_{\rm rp}(t)\dot{\Omega}_{\rm rs}(t)}{\Omega_{\rm rp}^2(t) + \Omega_{\rm rs}^2(t)}. \quad (26)$$

This approach facilitates the implementation of sa-STIRAP between dressed states in a three-level quantum system. We perform numerical simulations using the original Hamiltonian $H_8(t)$ (i.e., Eq. (20)) in the laboratory frame, without the rotating wave approximation. The parameter $t_{\rm f}$ is set to 1 μs, and the other parameters are consistent with those used in previous calculations. The results of sa-STIRAP are presented in Fig. 3(c) for Gaussian pulses and Fig. 3(d) for Vitanov-style pulses. By comparing these results with the STIRAP process shown in Figs. 3(a) and 3(b), it is evident that superadiabatic driving enhances the STIRAP process, especially when the adiabatic condition is not well satisfied.

Figure 4 shows the fidelity of the final state as a function of the total evolution time $t_{\rm f}$ for both the STIRAP and sa-STIRAP processes. The fidelity is defined as $F(t_{\rm f}) = |\langle g|\psi(t_{\rm f})\rangle|^2$. The inset provides a zoomed-in view of the fidelity for a shorter time interval. The results demonstrate that, for the STIRAP process, the fidelity of the state transfer approaches 1 when the total evolution time $t_{\rm f} > 3$ μs, while for the sa-STIRAP process, the fidelity approaches 1 when $t_{\rm f} > 0.1$ μs. The oscillations in the curves for $t_{\rm f} < 0.1$ μs are a result of numerical calculations performed without the rotating wave approximation.

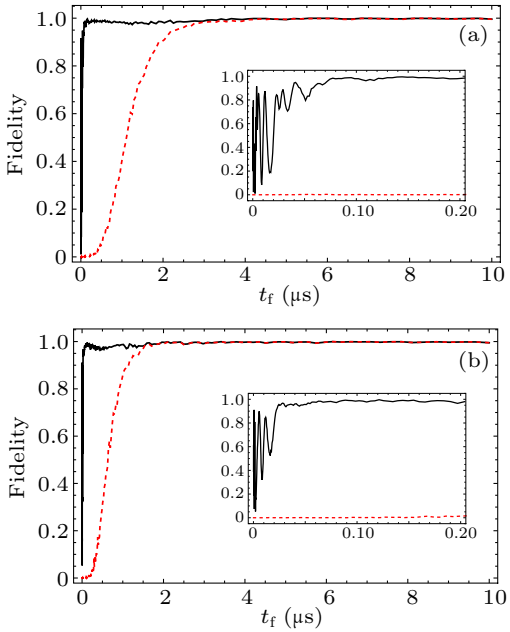


Fig. 4. The fidelity of the final state as a function of the total evolution time $t_{\rm f}$ in both the STIRAP and sa-STIRAP processes. The fidelity is defined as $F(t_{\rm f}) = |\langle g|\psi(t_{\rm f})\rangle|^2$. (a) Results obtained using Gaussian pulses. (b) Results obtained using Vitanov-style pulses. In each panel, the dashed red line represents the fidelity of the final state for the STIRAP process, while the solid black line represents the fidelity of the final state for the sa-STIRAP process. The inset shows a zoomed-in view of the fidelity for a shorter time interval, ranging from 0 μs to 0.2 μs.

5. Conclusion

In summary, we have introduced a novel method for implementing sa-STIRAP between dressed states. By modulating the amplitude and phase of the original driving fields, we demonstrate that the initial and target states in the dressed-state space can be effectively coupled, facilitating faster population transfer without the need for additional couplings that are typically required in traditional sa-STIRAP protocols. This approach offers a practical and experimentally feasible solution to the challenge of accelerating adiabatic state transfer, making sa-STIRAP more accessible for quantum systems in a variety of experimental setups.

Future research could focus on optimizing the driving field parameters further and investigating the robustness of this approach in the presence of noise and imperfections, which is essential for its practical implementation in real-world quantum devices. Moreover, this sa-STIRAP method could be applied to a variety of three-level quantum systems, including nitrogen-vacancy centers in diamond,[22,27,44] superconducting circuits,[24–26] cold atoms,[29,45,46] trapped ions,[47,48] and quantum dots.[49,50]

Acknowledgements

Project supported by the National Natural Science Foundation of China (Grant Nos. 12104282 and 12305014) and the Fundamental Research Funds for the Central Universities of China (Grant No. JZ2024HGTB0253).

References

[1] Gaubatz U, Rudecki P, Schiemann S and Bergmann K 1990 *J. Chem. Phys.* **92** 5363
[2] Bergmann K, Theuer H and Shore B W 1998 *Rev. Mod. Phys.* **70** 1003
[3] Vitanov N V, Rangelov A A, Shore B W and Bergmann K 2017 *Rev. Mod. Phys.* **89** 015006
[4] Vitanov N V, Halfmann T, Shore B W and Bergmann K 2001 *Ann. Rev. Phys. Chem.* **52** 763
[5] Král P, Thanopulos I and Shapiro M 2007 *Rev. Mod. Phys.* **79** 53
[6] Jing H 2008 *Chin. Phys. Lett.* **25** 847
[7] Zheng A S, Liu J B and Chen H Y 2011 *Chin. Phys. Lett.* **28** 080303
[8] Bergmann K, Vitanov N V and Shore B W 2015 *J. Chem. Phys.* **142** 170901
[9] Unanyan R G, Yatsenko L P, Bergmann K and Shore B W 1997 *Opt. Commun.* **139** 48
[10] Chen X, Lizuain I, Ruschhaupt A, Guéry-Odelin D and Muga J G 2010 *Phys. Rev. Lett.* **105** 123003
[11] Demirplak M and Rice S A 2003 *J. Chem. Phys. A* **107** 9937
[12] Demirplak M and Rice S A 2005 *J. Chem. Phys. B* **109** 6838
[13] Berry M V 2009 *J. Phys. A: Math. Theor.* **42** 365303
[14] Ruschhaupt A, Chen X, Alonso D and Muga J G 2012 *New J. Phys.* **14** 093040
[15] del Campo A 2013 *Phys. Rev. Lett.* **111** 100502
[16] Martínez-Garaot S, Torrontegui E, Chen X and Muga J G 2014 *Phys. Rev. A* **89** 053408
[17] Guéry-Odelin D, Ruschhaupt A, Kiely A, Torrontegui E, Martínez-Garaot S and Muga J G 2019 *Rev. Mod. Phys.* **91** 045001
[18] Li K Z, Tian J Z and Xiao L T 2024 *Phys. Rev. A* **109** 022443
[19] Li Y C and Chen X 2016 *Phys. Rev. A* **94** 063411
[20] Chen X and Muga J G 2012 *Phys. Rev. A* **86** 033405
[21] Baksic A, Ribeiro H and Clerk A A 2016 *Phys. Rev. Lett.* **116** 230503
[22] Zhou B B, Baksic A, Ribeiro H, Yale C G, Heremans F J, Jerger P C, Auer A, Burkard G, Clerk A A and Awschalom D D 2017 *Nat. Phys.* **13** 330
[23] Song X K, Meng F, Liu B-J, Wang D, Ye L and Yung M H 2021 *Opt. Express* **29** 7998
[24] Zheng W, Zhang Y, Dong Y, Xu J, Wang Z, Wang X, Li Y, Lan D, Zhao J, Li S and others 2022 *npj Quantum Information* **8** 9
[25] Kumar K S, Vepsäläinen A, Danilin S and Paraoanu G S 2016 *Nat. Commun.* **7** 10628
[26] Vepsäläinen A, Danilin S and Paraoanu G S 2019 *Sci. Adv.* **5** eaau5999
[27] Gong M, Yu M, Chu Y, Chen W, Cao Q, Wang N, Cai J, Betzholz R and Giannelli L 2024 *Phys. Rev. A* **109** 032626
[28] Giannelli L and Arimondo E 2014 *Phys. Rev. A* **89** 033419
[29] Du Y X, Liang Z T, Li Y C, Yue X X, Lv Q X, Huang W, Chen X, Yan H and Zhu S L 2016 *Nat. Commun.* **7** 12479
[30] Evangelakos V, Paspalakis E and Stefanatos D 2023 *Phys. Rev. A* **107** 052606
[31] Wilson C M, Duty T, Persson F, Sandberg M, Johansson G and Delsing P 2007 *Phys. Rev. Lett.* **98** 257003
[32] Timoney N, Baumgart I, Johanning M, Varón A F, Plenio M B, Retzker A and Wunderlich Ch 2011 *Nature* **476** 185
[33] Cai J M, Naydenov B, Pfeiffer R, McGuinness L P, Jahnke K D, Jelezko F, Plenio M B and Retzker A 2012 *New J. Phys.* **14** 113023
[34] Xu X, Wang Z, Duan C, Huang P, Wang P, Wang Y, Xu N, Kong X, Shi F, Rong X and Du J 2012 *Phys. Rev. Lett.* **109** 070502
[35] Belthangady C, Bar-Gill N, Pham L M, Arai K, Le Sage D, Cappellaro P and Walsworth R L 2013 *Phys. Rev. Lett.* **110** 157601
[36] Koshino K, Inomata K, Yamamoto T and Nakamura Y 2013 *Phys. Rev. Lett.* **111** 153601
[37] Golter D A, Baldwin T K and Wang H 2014 *Phys. Rev. Lett.* **113** 237601
[38] Teissier J, Barfuss A and Maletinsky P 2017 *J. Opt.* **19** 044003
[39] Xue Z Y, Gu F L, Hong Z P, Yang Z H, Zhang D W, Hu Y and You J Q 2017 *Phys. Rev. Appl.* **7** 054022
[40] Barfuss A, Kölbl J, Thiel L, Teissier J, Kasperczyk M and Maletinsky P 2018 *Nat. Phys.* **14** 1087
[41] Kölbl J, Barfuss A, Kasperczyk M S, Thiel L, Clerk A A, Ribeiro H and Maletinsky P 2019 *Phys. Rev. Lett.* **122** 090502
[42] Jin F, Geng J and Zhou H 2025 *Phys. Rev. A* **111** 022620
[43] Vasilev G S, Kuhn A and Vitanov N V 2009 *Phys. Rev. A* **80** 013417
[44] González F J and Coto R 2022 *Quantum Science and Technology* **7** 025015
[45] Du Y X, Liang Z T, Huang W, Yan H and Zhu S L 2014 *Phys. Rev. A* **90** 023821
[46] Ling K, Jiang L, Wan R G and Yao Z H 2023 *Chin. Phys. B* **32** 044211
[47] Sørensen J L, Møller D, Iversen T, Thomsen J B, Jensen F, Staanum P, Voigt D and Drewsen M 2006 *New J. Phys.* **8** 261
[48] Zhang J W, Bu J T, Li J C, Meng W, Ding W Q, Wang B, Yuan W F, Du H J, Ding G Y, Chen W J, Chen L, Zhou F, Xu Z and Feng M 2024 *Phys. Rev. Lett.* **132** 213602
[49] Fountoulakis A and Paspalakis E 2013 *J. Appl. Phys.* **113** 174301
[50] Liu X F, Matsumoto Y, Fujita T, Ludwig A, Wieck A D and Oiwa A 2024 *Phys. Rev. Lett.* **132** 027002